arXiv:nucl-th/9801041v1 21 Jan 1998

TUM/T39-98-1

Coherent Vector Meson Production from Deuterons

L. Frankfurt[a,d], G. Piller[b], M. Sargsian[b,e], M. Strikman[c,d]

(a) School of Physics and Astronomy, Tel Aviv University, Tel Aviv, 69978 Israel
(b) Physik Department, Technische Universität München, D-85747 Garching, Germany
(c) Pennsylvania State University, University Park, PA 16802, USA
(d) Institute for Nuclear Physics, St. Petersburg, Russia
(e) Yerevan Physics Institute, Yerevan 375036, Armenia

Abstract

In this paper we discuss coherent photo- and leptoproduction of vector mesons from deuterons at intermediate (virtual) photon energies, $3 \leq \nu \leq 30\,GeV$. We consider the scattering from unpolarized and polarized targets as well as processes where the polarization of the recoil deuteron is measured. Our main motivation results from the need for a quantitative analysis of the space-time structure of photon-induced processes. In this respect we suggest several possibilities to explore the characteristic longitudinal interaction length in coherent vector meson production. Furthermore, we outline methods for an investigation of color coherence effects. Besides the presentation of benchmark values for the maximal possible color coherence effect in various kinematic regions, we illustrate the anticipated phenomena within the color diffusion model. Finally we recall that the determination of vector meson-nucleon cross sections is not a closed issue. Besides being not known to a satisfying accuracy, they can be used to determine the strength of the D-state in low mass vector mesons.

1 Introduction

Exclusive vector meson production from nucleons and nuclei can be used to investigate the transition from non-perturbative to perturbative strong interaction mechanisms. To identify different kinematic domains we consider the scattering of a (virtual) photon with four-momentum $q^\mu = (\nu, \boldsymbol{q})$ from a nucleon. ($Q^2 = -q^2$, M stands for the invariant mass of the nucleon target, and $x = Q^2/2M\nu$ is the Bjorken scaling variable in the lab frame.) At $\nu \geq 3\,GeV$ and $x \leq 0.1$ one can decompose the amplitude for the production of a vector meson V in terms of hadronic Fock states of the (virtual) photon (see e.g. [1, 2]):

$$f^{\gamma^* N \to VN} = \sum_h \frac{< 0|\epsilon_{\gamma^*} \cdot J^{em}|h > d\tau_h}{E_h - \nu} f^{hN \to VN}. \tag{1}$$

Here ϵ_{γ^*} is the polarization vector of the virtual photon, and J^{em} denotes the electromagnetic current. E_h stands for the energy of the intermediate hadronic state h with phase space $d\tau_h$.

At intermediate photon energies $3 \leq \nu \leq 30\,GeV$ and low momentum transfers $Q^2 \lesssim 1\ GeV^2$ contributions to $f^{\gamma^* N \to VN}$ from hadronic Fock states with large invariant mass m_h are suppressed by large energy denominators $E_h - \nu \approx (m_h^2 + Q^2)/(2\nu)$ (and small photon-hadron couplings). The restriction to light intermediate hadronic states leads to vector meson dominance (VMD). Here, as seen from the laboratory frame, the vector meson is formed prior to the interaction with the target (see e.g. [1, 3]).

This is different at large momentum transfers $Q^2 \gg 1\ GeV^2$ and $x \ll 0.1$. Here it is legitimate to use closure over intermediate hadronic states h and substitute the sum over hadronic states in Eq.(1) by quark-gluon Fock states which can be calculated in the framework of perturbative QCD. For example, in the case of longitudinally polarized photons short distance dominance leads at large Q^2 to the production of color-dipole quark-antiquark pairs with small transverse size [4, 5, 6, 7]. Long after this initial hard interaction the final state vector meson is formed.

Interesting details about the production process can be obtained by embedding it into nuclei. Here details about the initially produced quark-gluon wave packet and the formation of the finally measured vector meson are probed via the interaction with spectator nucleons (for recent reviews see e.g. [8]). In this context we discuss coherent photo- and leptoproduction of vector mesons from deuterons at photon energies $3 \leq \nu \leq 30\,GeV$ and $0 \leq Q^2 \leq 10\,GeV^2$. In this kinematic regime one is most sensitive to the transition from non-perturbative to perturbative production mechanisms. The corresponding amplitudes can be split into two pieces: a single scattering term in which only one nucleon participates in the interaction, and a double scattering contribution. Here the photon interacts with one of the nucleons inside the target and produces an intermediate hadronic state which subsequently re-scatters from the second nucleon before forming the final state vector meson.

In the considered process the following scales seem to be most relevant: the average **transverse size** of the wave packet which for the case of longitudinal photons is $b_{ej} \approx 4 \ldots 5/Q$ for the contribution of the minimal Fock space component at $Q^2 \gtrsim 5GeV^2$ [5]. For

these Q^2 it amounts to less than a third of the typical diameter of a ρ meson ($b_\rho \approx 1.4\,fm$). Furthermore, the initially produced small quark-gluon wave packet does not, in general, represent an eigenstate of the strong interaction Hamiltonian. The finally measured vector meson is formed after a typical **formation time** $\tau_f \approx 2\nu/\delta m_V^2$. Here $\delta m_V^2 \sim 1\,GeV^2$ is the characteristic difference of the squared masses of low-lying vector meson states. For energies $\nu \simeq 10\,GeV$ one finds $\tau_f \simeq 4\,fm$. Therefore in the considered kinematic region details about the expansion of the initially produced wave packet are expected to significantly influence the production of vector mesons from nuclei. The kinematic dependence of the initial transverse size of the produced wave packet and the formation time of the final vector meson suggest that contributions from re-scattering processes decrease at large photon energies with rising Q^2. This phenomenon is commonly called color coherence or color transparency [8].

However dominant contributions to high-energy, photon-induced processes result from large longitudinal space-time intervals which increase with the photon energy [1, 9, 10]. In the considered kinematic domain the characteristic **longitudinal interaction length** $\lambda \approx 2\nu/(m_V^2 + Q^2)$ turns out to be of the order of typical nuclear dimensions and can have a major influence on the scattering process. A systematic investigation of the role of the longitudinal interaction length is most important, even for a qualitative understanding of photon-induced processes.

In a previous publication [11] we have focussed mainly on the derivation of vector meson production amplitudes. In this paper we collect several possibilities which can be used for a detailed investigation of the space-time structure of vector meson production. Furthermore, we illustrate the anticipated color coherence effect in the framework of the quantum diffusion model [12]. Finally we recall that the determination of vector meson-nucleon cross sections is not a closed issue. Despite many experimental studies they are not known to a satisfying accuracy. Furthermore, we point out that for polarized vector mesons they can be used to determine the strength of the D-state component in low mass vector mesons.

This paper is organized as follows: we recall in Sec.2 the photon-deuteron scattering amplitude. In Sec.3 we discuss various possibilities for an investigation of the longitudinal interaction length in coherent vector meson production. Different signatures for color coherence are explored in Sec.4. In Sec.5 we comment on measurements of vector meson-nucleon cross sections. Finally we summarize.

2 Photon-deuteron scattering amplitude

Let us briefly recall the vector meson production amplitude for a deuteron target. Throughout this work we stay in the laboratory frame where the deuteron with invariant mass M_d is at rest. Furthermore, we choose the photon momentum in the longitudinal direction, i.e. $q^\mu = (\nu, \mathbf{0}_\perp, \sqrt{Q^2+\nu^2})$. The single scattering, or Born amplitude reads [11]:

$$F_1^j \;=\; f^{\gamma^* p \to V p}(\boldsymbol{l})\, S_d^j\left(-\frac{\boldsymbol{l}_\perp}{2}, \frac{l_-}{2}\right) \;+\; f^{\gamma^* n \to V n}(\boldsymbol{l})\, S_d^j\left(\frac{\boldsymbol{l}_\perp}{2}, -\frac{l_-}{2}\right). \qquad (2)$$

It is determined by the vector meson production amplitude $f^{\gamma^* p(n)\to V p(n)}$ from a proton or neutron, respectively, and the deuteron form factor S_d^j, where j labels the dependence on the target polarization. The transfered momentum is denoted by $l^\mu = (l_0, \boldsymbol{l}) = q^\mu - k_V^\mu$ with k_V, the momentum of the produced vector meson. Note that Eq.(2) corresponds to the well known result of Refs.[19, 20] derived in the eikonal approximation, except for the presence of $l_- = l_0 - l_z = \sqrt{M_d^2 + \boldsymbol{l}^2} - M_d - l_z$ in the form factor which accounts for the recoil of the two-nucleon system (for a derivation see [11]).

In the eikonal approximation the dominant contribution to the double scattering amplitude is given by [11]:

$$F_2^j \;\approx\; \frac{i}{2}\sum_h \int \frac{d^2k_\perp}{(2\pi)^2}\, S_d^j(\boldsymbol{k}_\perp, -\Delta_h) f^{\gamma^* N\to hN}\left(\frac{\boldsymbol{l}_\perp}{2} - \boldsymbol{k}_\perp\right) f^{hN\to VN}\left(\frac{\boldsymbol{l}_\perp}{2} + \boldsymbol{k}_\perp\right). \quad (3)$$

Here $\Delta_h = (Q^2 + 2m_h^2 - m_V^2 + t)/(4\nu)$, with the invariant mass m_h of the intermediate hadronic state, and $t = l^2$. In Eq.(3) we have neglected any isospin dependence of nucleon amplitudes.

The differential cross section for coherent vector meson production in (virtual) photon-deuteron interactions finally reads:

$$\frac{d\sigma^j_{\gamma^{(*)}N}}{dt} = \frac{1}{16\pi}\left(|F_1^j|^2 + 2Re\left(F_1^{j*}F_2^j\right) + |F_2^j|^2\right). \quad (4)$$

We have not yet specified the polarization of the incident photon. Contrary to real photoproduction, where only transversely polarized photons (γ_T) enter, in leptoproduction also contributions from the exchange of longitudinal photons (γ_L) arise. The leptoproduction cross section can therefore be split according to:

$$\frac{d\sigma^j_{lN}}{dQ^2 d\nu dt} = \Gamma_V \frac{d\sigma^j_{\gamma^* N}}{dt} = \Gamma_V\left(\frac{d\sigma^j_{\gamma_T^* N}}{dt} + \varepsilon\,\frac{d\sigma^j_{\gamma_L^* N}}{dt}\right). \quad (5)$$

Here Γ_V is related to the flux of the virtual photon:

$$\Gamma_V = \frac{\alpha_{em}}{2\pi}\frac{K}{Q^2}\frac{1}{E_e^2}\frac{1}{1-\epsilon}, \quad (6)$$

where $\alpha_{em} = 1/137$ is the electromagnetic coupling constant and $K = \nu(1-x)$. The parameter $\epsilon = (4E_eE_e' - Q^2)/(2(E_e^2 + E_e'^2) + Q^2)$ specifies the photon polarization and is determined by the incoming and scattered lepton energies E_e and E_e'.

In the following we investigate the differential cross section $d\sigma^j_{\gamma^{(*)}N}/dt$ for various target polarizations j. For this purpose we have to specify the nucleon amplitudes which enter in Eqs.(2,3). In this respect we should mention that we assume s-channel helicity conservation throughout this work.

2.1 Vector meson dominance

In the kinematic domain of vector meson dominance ($Q^2 \lesssim 1\,GeV^2$ and $\nu \geq 3\,GeV$) the vector meson production amplitude for transverse photons is successfully parametrized as [3]:

$$f^{\gamma_T^* N \to VN} \approx \frac{\sqrt{\alpha_{em}\pi}}{g_V} \frac{m_V^2}{m_V^2 + Q^2} f^{V_T N \to VN}. \tag{7}$$

Here V_μ ($V = \rho, \omega, \phi$) stands for a vector meson with invariant mass m_V and coupling constant g_V, and $f^{V_T N \to VN}$ denotes the amplitude for the elastic scattering of a transversely polarized vector meson from a nucleon. The amplitude for longitudinal photons is given by:

$$f^{\gamma_L^* N \to VN} = \xi \frac{\sqrt{Q^2}}{m_V} f^{\gamma_T^* N \to VN}, \tag{8}$$

where $\xi = f^{V_L N \to VN}/f^{V_T N \to VN}$ is the ratio of the longitudinal and transverse vector meson scattering amplitudes.

It remains to fix the amplitude $f^{\gamma_T^* N \to VN}$. We illustrate most of the discussed issues for the case of ρ production and use the parametrization:

$$f^{\gamma_T^* N \to \rho N} = A(i + \alpha) e^{\frac{B(Q^2)}{2} t}, \tag{9}$$

with $A = \sigma_{V_T N} \sqrt{\alpha_{em}\pi} m_V^2/((m_V^2 + Q^2) g_V)$. In real photoproduction of ρ mesons one finds at $\nu = 17\,GeV$ typically $A \approx 68\,\mu b$ [3]. For the slope $B(Q^2)$ we use the empirical values [3, 21]: $B(Q^2 < 1\,GeV^2) = 7\,GeV^{-2}$, $B(1 < Q^2 < 2\,GeV^2) = 6\,GeV^{-2}$, and $B(2 < Q^2 < 10\,GeV^2) = 5\,GeV^{-2}$. The ρ-nucleon amplitude is then obtained from Eq.(7) using the slope $B \approx 8\ GeV^{-2}$. Furthermore we take $\xi^2 = 0.5$ [3]. The real part of the amplitude in Eq.(9) can be estimated at high energies through an empirical relation between the amplitudes for ρ photoproduction and elastic pion-nucleon scattering:

$$f^{\gamma p \to \rho p} \sim f^{\pi^+ p \to \pi^+ p} + f^{\pi^- p \to \pi^- p}. \tag{10}$$

From a compilation of π-proton scattering data at the considered energies one obtains $\alpha \approx -0.2$ [13]. This corresponds to a decrease of the ρ-proton cross section with rising center of mass energies (see e.g. [14]) as described by contributions from secondary Regge trajectories. Note that the situation is different for ϕ production. In the considered kinematic region the corresponding production cross section increases with the center of mass energy s. From the Gribov relation [15],

$$Ref(s, t = 0) = \frac{\pi}{2} \frac{d\, Imf(s, t = 0)}{d \log s}, \tag{11}$$

one finds $\alpha = 0.13$. In the following we neglect any t-dependence of α.

It should be mentioned that Regge trajectories which correspond to isospin exchange are not important for isoscalar targets as the deuteron. In the Born approximation such contributions vanish exactly.

2.2 Quantum diffusion

To illustrate the anticipated implications of color coherence in vector meson production at large $Q^2 \gg 1\,GeV^2$ we employ the quantum diffusion model [12]. It describes in a simplified manner the evolution and re-scattering of a quark-gluon wave packet which is produced in the initial (virtual) photon-nucleon interaction. For ρ production the corresponding re-scattering amplitude is given by [22]:

$$f^{ej}(z,t,Q^2) = i\sigma_{ej}(z,Q^2)\exp\left\{\frac{B}{2}t + \frac{b_\rho^2}{6}\left(\frac{\sigma_{ej}(z,Q^2)}{\sigma_{\rho N}} - 1\right)t\right\}. \tag{12}$$

The interaction cross section of the quark-gluon wave packet at a longitudinal distance z from its initial production point is [12]:

$$\sigma_{ej}(z,Q^2) = \sigma_{\rho N}\left\{\left(\frac{z}{\tau_f} + \frac{b_{ej}^2(Q^2)}{b_\rho^2}\left(1 - \frac{z}{\tau_f}\right)\right)\Theta(\tau_f - z) + \Theta(z - \tau_f)\right\}. \tag{13}$$

As already discussed in the introduction, σ_{ej} is determined by the transverse size of the initially produced ejectile, $b_{ej}(Q^2) \sim 1/Q$, and the characteristic formation time τ_f of the vector meson. For distances larger than τ_f it coincides with the ρ meson-nucleon cross section $\sigma_{\rho N} \approx 27\,mb$ [3].

Another class of models describes the production of vector mesons within a hadronic basis including nondiagonal transitions between different intermediate hadronic states (see e.g. [16, 17, 18]). Here re-scattering is controlled by the destructive interference between diagonal (elastic) and nondiagonal (diffractive dissociation) transitions in meson-nucleon scattering processes. For the production of ground state vector mesons the results of such models are qualitatively similar to the considered quantum diffusion picture.

3 Probing the longitudinal interaction length

High energy photon-induced processes are dominated by contributions from large longitudinal space-time intervals. For coherent vector meson production characteristic distances can be extracted from the production amplitudes in Eqs.(2,3) after a Fourier transformation into coordinate space. The obtained length scales are to a good approximation inversely proportional to the longitudinal momentum transfers which enter in the form factors in Eqs.(2,3). For single scattering one finds:

$$\delta_1 \sim \left|\frac{1}{l_-}\right| = \frac{2\nu}{Q^2 + m_V^2 - t}. \tag{14}$$

Note that if the deuteron recoil is neglected one obtains $\delta_1 \sim |1/l_z| = 2\nu/(Q^2 + m_V^2 - t - \nu t/2M)$, which becomes constant at high energies. This, however, is in contradiction with our basic understanding of high-energy photon-induced processes being controlled by longitudinal distances which increase with the photon energy ν [1, 9, 10, 23].

For double scattering we obtain from Eq.(3):

$$\delta_2 \sim \left|\frac{1}{-2\Delta_V}\right| = \left|\frac{2\nu}{Q^2 + 2\langle m_h^2\rangle - m_V^2 + t}\right|, \tag{15}$$

where $\langle m_h^2\rangle$ stands for the average squared mass of the intermediate hadronic states.

In the following we discuss several possibilities for a detailed investigation of the characteristic longitudinal interaction length in vector meson production. For this purpose one has to concentrate on kinematic regions where distances of the order of the target size, $\delta_1, \delta_2 \sim \langle r^2\rangle_d^{1/2}$, are reached. Up to now investigations of this kind have not been carried out, although the presence of significant nuclear effects due to a non-vanishing longitudinal interaction length has been observed in shadowing effects in total photon-nucleus scattering cross sections (see e.g. [24]). In particular we want to emphasize that the non-trivial t-dependence of the longitudinal interaction length in Eqs.(14,15), which has been derived in Ref.[11], needs to be verified to complete our understanding of photon-induced processes.

3.1 Photoproduction from unpolarized deuterons

At moderate photon energies $\nu \gtrsim 3\,GeV$, as available at TJNAF, the longitudinal interaction distance for single scattering (14) is for small values of the momentum transfer t typically of the order of the deuteron size. For example at $\nu = 4\,GeV$ and $t = -0.2\,GeV^2$ one finds $\delta_1 \approx 2\,fm$. Consequently in this kinematic region, which is governed by the Born contribution, a strong dependence of the production cross section on ν is expected. To illustrate this issue consider the ρ meson photoproduction cross section (4) calculated within vector meson dominance. It is important to use proper longitudinal interaction distances (14, 15) as they appear in the scattering amplitude (2,3). We normalize our results by the production cross section obtained in the limit $\delta_1, \delta_2 \to \infty$. The corresponding ratio

$$R_\delta = \frac{d\sigma_{\gamma N}}{dt} \Big/ \frac{d\sigma_{\gamma N}}{dt}(l_- = \Delta_\rho = 0). \tag{16}$$

is shown in Fig.1a for various photon energies. At $t \simeq -0.1\,GeV^2$ we indeed observe a 15% rise of R_δ for an increase of the photon energy from 3 to $6\,GeV$. At large $-t > 0.7\,GeV^2$, where double scattering dominates, only minor variations of the production cross section occur. This is due to the fact that the corresponding interaction length is larger than for single scattering. Thus the difference in the t-dependence of the longitudinal interaction length for single and double scattering reveals itself through a different pattern in the energy dependence of the production cross section at small and large $|t|$. For other low-mass vector mesons similar effects are expected.

3.2 Polarized deuterons

The coherent photoproduction of vector mesons from polarized deuterons or, equivalently, a measurement of the polarization of the recoil deuteron provides further possibilities to

investigate effects due to a change of the characteristic longitudinal interaction length. If the polarization of the scattered or recoil deuteron, respectively, is chosen parallel to the photon momentum $\boldsymbol{q}$ one finds for the single scattering cross section:

$$\left.\frac{d\sigma^{\parallel}_{\gamma N}}{dt}\right|_{Born} \sim \left(F_C(\tilde{l}/2) - \frac{F_Q(\tilde{l}/2)}{\sqrt{2}}\right)^2 + \frac{3l_-^2}{2\tilde{l}^2} F_Q(\tilde{l}/2)\left(2\sqrt{2}F_C(\tilde{l}/2) + F_Q(\tilde{l}/2)\right), \qquad (17)$$

where $\tilde{l}^2 = \boldsymbol{l}_\perp^2 + l_-^2$. F_C and F_Q are the deuteron monopole and quadrupole form factors [25]. The first term in Eq.(17) vanishes at $\tilde{l} \approx 0.7\,GeV$, while the second, which is proportional to $l_-^2 \sim 1/\delta_1^2$, decreases for increasing photon energies. As a consequence the Born contribution to the production cross section develops a node at $t \approx -0.5\,GeV^2$. Therefore in this kinematic region a strong energy dependence of the production cross section is expected. Note that the energy dependence of the second term in Eq.(17) is a consequence of the particular choice of the deuteron polarization being parallel to the photon momentum.

In Fig.2 we show the differential ρ meson photoproduction cross section calculated within vector meson dominance for various photon energies. The significant energy dependence of the Born contribution at $t \approx -0.5\,GeV^2$ leads to a decrease of the full production cross section at $t \approx -0.35\,GeV^2$ of more than two orders of magnitude, if the photon energy rises from $\nu = 3$ to $20\,GeV$. In previous treatments of photoproduction processes at small t the longitudinal interaction length was taken to be proportional to the inverse momentum transfer $\delta_1 \sim |1/l_z|$ neglecting any t-dependence [3]. Within this approximation the above discussed node in the differential cross section would be absent, even at large photon energies. Therefore polarized deuteron targets or, equivalently, a measurement of the polarization of the recoil deuteron allow a detailed investigation of the kinematic dependence of the longitudinal interaction length.

3.3 Leptoproduction from unpolarized deuterons

In high-energy leptoproduction processes the longitudinal interaction lengths $\delta_{1,2}$ (15,14) exhibit a characteristic Q^2-dependence. At moderate values of $0.5 \lesssim Q^2 \lesssim 2\,GeV^2$, as available at TJNAF, variations of $\delta_{1,2}$ of the order of the target size are expected. Therefore a strong Q^2-dependence of vector meson production is anticipated. In the framework of vector meson dominance this is visualized in Fig.1b. We show the cross section ratio R_δ from Eq.(16) for various Q^2 at a fixed photon energy $\nu = 6\,GeV$. Indeed we observe at $t \approx -0.1\,GeV^2$ a decrease of R_δ by approximately 50%, if Q^2 rises from 0.5 to $2\,GeV^2$.

Similar effects are expected at higher photon energies. Then – to keep the typical longitudinal interaction length close to the target size – larger values of Q^2 are needed. For example at HERMES energies, $\nu \approx 25\,GeV$, values of $Q^2 \approx (2{-}10)\,GeV^2$ are required. To avoid complications due to color coherence effects one has to focus on the kinematic domain where the Born contribution dominates, i.e. $-t \lesssim 0.4\,GeV^2$.

4 Search for color coherence

In this section we focus on the possibility to study color coherence effects in coherent vector meson production from deuterons. For this purpose one needs to investigate the Q^2-dependence of the corresponding cross section in kinematic regions where it is most sensitive to re-scattering. However it is mandatory to account for possible modifications due to changes of the characteristic longitudinal interaction lengths δ_1 and δ_2 from Eqs.(14,15). Or, even better, the kinematics should be chosen such that these length scales stay reasonably constant. For $Q^2 > 1\,GeV^2 > m_V^2, |t|$ this can be achieved in an approximate way by keeping the Bjorken scaling variable fixed. It should be mentioned that in vector meson production the onset of color coherence might occur already at moderate values of $Q^2 \gtrsim 1\,GeV^2$. This expectation is based on the observation that the vector current correlation function assumes its perturbative form already at relatively large distances [26]. Furthermore, large size fluctuations of the minimal wave function of longitudinally polarized photons are suppressed by a factor $1/Q^2$ as compared to the transverse case (see e.g. [4]). Therefore color coherence effects should arise earlier in the longitudinal channel.

We illustrate our investigations for the case of ρ meson production. The obtained results can be applied, however, to other vector mesons too. Differences in the onset of color coherence for various vector mesons and their excited states are expected (see e.g. [12]). They should result from differences in the mass scales which are involved in the hard interaction, as well as from deviations between the wave functions of the final state vector mesons. An experimental investigation of these issues is certainly needed.

4.1 Unpolarized deuteron targets

The maximal signal which can result from color coherence is determined by the difference between the Born cross section, which results from single scattering only, and the full production cross section at $Q^2 \approx 0$. In Fig.3 we show the ratio of the full ρ production cross section and the Born term for various values of t at $x = 0.1$:

$$R_{ct} = \left(\frac{d\sigma_{\gamma^* N}}{dt}\right) \Big/ \left(\frac{d\sigma_{\gamma^* N}}{dt}\right)_{Born} . \tag{18}$$

We have applied the quantum diffusion model from Sec.2.2 using a characteristic formation time τ_f as determined by the mass difference $\delta m_\rho^2 \approx 0.7\,GeV^2$. Color coherence effects are calculated for two different scenarios: (i) color coherence applies to transversely and longitudinally polarized photons equally; (ii) color coherence affects only the longitudinal cross section but not the transverse one. In the second case the cross section ratio is calculated for a photon polarizations (5) characterized by $\varepsilon = 0.5$.

At small values of $t \simeq -0.1\,GeV^2$ single scattering dominates and color coherence effects are small. Double scattering starts to become relevant already at moderate $t \gtrsim -0.2\,GeV^2$. Here the interference of the double and single scattering amplitude is important. For real photoproduction it results in a cross section smaller than the Born piece. Consequently

here color coherence leads to an increase of the cross section ratio R_{ct} with rising Q^2. At large $|t|$ coherent photoproduction of vector mesons is dominated by double scattering. Therefore in this region color coherence implies a decrease of R_{ct} at large Q^2. Note that even if we omit color coherence effects for transversely polarized photons, the Q^2-dependence of the virtual photoproduction cross section remains nearly unchanged.

The difference between the full cross section and the Born piece can be enhanced if one considers the ratio of cross sections at large and moderate $|t|$. Here any Q^2-dependence, apart from being caused by color coherence, cancels to a large extent. In Fig.4 we present the ratio of the ρ meson production cross sections taken at $x = 0.1$ for $t = -0.4\,GeV^2$ and $t = -0.8\,GeV^2$. The Born cross section and the full vector meson dominance calculation differ by a factor four, leaving reasonable room for an investigation of color coherence. We also present results obtained from the quantum diffusion model, assuming similar color coherence effects for longitudinal and transverse photons. To emphasize the strong dependence of the measured cross section ratio on the expansion mechanism of the initial wave packet we vary δm_ρ^2 between 0.7 and $1.1\,GeV^2$. The observed sensitivity is due to the moderate photon energies considered. On the other hand variations of the initial size of the wave packet do not change our results significantly, e.g. a 30% rise in b_{ej} changes the cross section ratio over the entire range of Q^2 by less than 5%.

4.2 Polarized deuterons

At moderate values of $|t|$ vector meson production from unpolarized deuterons is largely dominated by the Born contribution. If the polarization of the target, or alternatively, of the scattered deuteron is fixed even here kinematic windows exist where the Born contribution is small and the production cross section becomes sensitive to re-scattering.

A promising signature for color coherence can be obtained by choosing the polarization of the target or the scattered deuteron, respectively, perpendicular to the vector meson production plane, i.e. parallel to $\boldsymbol{q} \times \boldsymbol{l}$. The corresponding Born cross section is then proportional to:

$$\left.\frac{d\sigma^{\perp}_{\gamma^* N}}{dt}\right|_{Born} \sim \left(F_C^2(\tilde{l}/2) - \frac{1}{\sqrt{2}} F_Q(\tilde{l}/2)\right)^2 , \tag{19}$$

irrespective of the magnitude of the longitudinal momentum transfer l_-. Consequently a node in the Born contribution occurs for $\tilde{l} = 0.7\,GeV$, which corresponds at large photon energies approximately to $t \approx -0.5\,GeV^2$. In Fig.5 we show the t-dependence of the ρ production cross section normalized to its value at $t = t_{min}$ for various values of Q^2 but fixed $x = 0.1$. We present results from vector meson dominance and quantum diffusion. With rising Q^2 one observes a considerable decrease of the production cross section at $-t \gtrsim 0.4$, and a shift of the cross section minimum towards the node in the single scattering cross section at $t \approx -0.5\,GeV^2$.

Finally we consider the cross section for tensor polarization normalized by the unpo-

larized production cross section:

$$A_d = \frac{d\sigma^{m=1}/dt + d\sigma^{m=-1}/dt - 2d\sigma^{m=0}/dt}{d\sigma/dt}. \tag{20}$$

We choose the spin quantization axis either perpendicular to the vector meson production plane or parallel to the photon momentum. In comparison to the corresponding asymmetry for the Born contribution we find a significant sensitivity to double scattering at $-t \geq 0.6\,GeV^2$ as demonstrated in Fig.6. Here color coherence leads to a sign-change of A_d.

5 Vector meson-nucleon cross sections

We have illustrated above how coherent vector meson production from deuterons can be used for a detailed investigation of color coherence effects. In a similar way it can be employed at low Q^2 to determine the interaction cross sections of vector mesons. Their precise knowledge is relevant for various topics in strong interaction physics, ranging from the investigation of hadron production processes to the analysis of nucleus-nucleus collisions. Despite a long history of experimental studies (see e.g. [3, 14]) ω-, ϕ- and ψ-nucleon cross sections are not known to satisfactory accuracy. In particular we should mention that in the case of ψ-mesons and probably to some extend also ϕ mesons their extraction from photoproduction processes off nucleons in the framework of vector meson dominance is likely to give too small values (for an early discussion see e.g. [27]).

This situation can be improved through an investigation of coherent vector meson production at low $Q^2 \lesssim 0.5\,GeV^2$ in kinematic regions dominated by double scattering processes which have been discussed in the previous section. While unpolarized targets require a large momentum transfer, polarized targets allow such investigations already at moderate t (see Sec.4.2). For illustration we discuss ϕ meson production. In Fig.7 we show the polarized photoproduction cross section $\sigma^{\perp}_{\gamma N}/dt$ normalized to its value at $t = t_{min}$ for two different ϕ-nucleon interaction cross sections $\sigma_{\phi N} = 10$ and $15\,mb$. The photon energy is fixed at $6\,GeV$. At $t \simeq -0.45\,GeV^2$, where double scattering is important, we observe a significant sensitivity on $\sigma_{\phi N}$. Here both production cross sections differ approximately by one order of magnitude.

Finally let us mention that vector meson-nucleon cross sections for polarized vector mesons carry interesting information too. In the framework of quark models mesons are considered as bound states of a quark and antiquark (see e.g. [28]). Since vector mesons carry spin 1, the $q\bar{q}$ pair can be in a S- or D-state. The latter, however, is of asymmetric shape. In leptoproduction a smaller than average configuration of the vector meson wave function is selected due to the involved mass difference. If the probed wave function component contains a significant D-state contribution, a difference in the rescattering process for longitudinally and transversely polarized vector mesons is expected. Thus polarized leptoproduction of vector mesons at low $Q^2 \lesssim 0.5 GeV^2$ can give interesting information about the strength of the corresponding D-state component.

6 Summary

The space-time structure of exclusive production processes contains valuable information on the transition from non-perturbative to perturbative strong interaction mechanisms. Especially the use of nuclear targets is of advantage since here the production process is probed at a typical length scale of around $2\,fm$, as given by the average nucleon-nucleon distance.

We have outlined several possibilities to investigate the characteristic longitudinal interaction length of photon-induced processes. Such a study has never been performed on a quantitative level. In this context we have stressed in particular the non-trivial dependence of the longitudinal interaction length on the momentum transfer t. This genuine new effect could be explored to great detail at TJNAF – especially with polarized targets or deuteron polarimeters (e.g. at TJNAF Hall C).

Furthermore, we have explored possibilities to investigate color coherence effects. Promising signatures have been presented at moderate and large momentum transfers. We have illustrated the anticipated color coherence effects within the color diffusion model. At the considered energies a large sensitivity to details on the formation of the final vector meson has been observed.

Finally we recall that the determination of vector meson-nucleon cross sections is not a closed issue. Besides being not known to a satisfying accuracy, they can be used to determine the strength of the D-state in low mass vector meson states.

Acknowledgments

We would like to thank G. van der Steenhoven and Eric Voutier for discussions.
This work was supported in part by the German-Israeli Foundation Grant GIF -I-299.095, the U.S. Department of Energy under Contract No. DE-FG02-93ER40771, and the BMBF. M. Sargsian is grateful to the Alexander von Humboldt Foundation for support. Three of us (G.P., M.S. and M.S.) enjoyed the kind hospitality of the Institute of Nuclear Theory, Seattle, during the preparation of this paper.

References

[1] V.N. Gribov, JETP **30** (1970) 709.

[2] R.D. Spital and D.R. Yennie, Nucl. Phys. **106** (1976) 269 .

[3] T.H. Bauer, R.D. Spital, D.R. Yennie and F.M. Pipkin, Rev. Mod. Phys. **50** (1978) 261.

[4] S.J. Brodsky, L.L. Frankfurt, J.F. Gunion, A.H. Mueller and M.I. Strikman, Phys. Rev. **D50** (1994) 3134.

[5] L.L. Frankfurt, W. Koepf and M.I. Strikman, Phys. Rev. **D54**, (1996) 3194.

[6] H. Abramowicz, L.L. Frankfurt and M.I. Strikman, DESY-95047, 1995.

[7] L.L. Frankfurt, V. Guzey, W. Koepf, M. Sargsian and M.I. Strikman, *Proceedings of the Workshop "Future Physics at HERA"*, 1996, Vol.II, p.946

[8] L.L. Frankfurt, G.A. Miller and M.I. Strikman, Ann. Rev. Nucl. Part. Sci. **45** (1994) 501; P. Jain, B. Pire and J.P. Ralston, Phys. Rep. **271** (1995) 133.

[9] V.N. Gribov, B.L. Ioffe and I.Ya. Pomeranchuk, Soviet Journal of Nucl. Phys. **2** (1966) 549; B.L. Ioffe, Phys. Lett. 30 (1968) 123.

[10] C. Llewellyn-Smith, Phys. Rev. **D4** (1971) 2392.

[11] L.L. Frankfurt, J. Mutzbauer, W. Koepf, G. Piller, M. Sargsian and M.I. Strikman, Nucl. Phys. A **662** (1997) 511.

[12] G.R. Farrar, L.L. Frankfurt, M.I. Strikman and H. Liu, Phys. Rev. Lett. **61** (1988) 686.

[13] M. Kamran, Phys. Rep. **108** (1984) 275.

[14] J.A. Crittenden, Springer Tracts in Modern Physics, **140** (1997) 100.

[15] V.N. Gribov, Sov. Phys. JETP **26** (1968) 414.

[16] H. Fraas, B.J. Read and D. Schildknecht, Nucl. Phys. **B88** (1975) 301.

[17] A. Donnachie and G. Shaw, *Electromagnetic Interactions of Hadrons Vol. 2*, edited by A. Donnachie and G. Shaw (Plenum, New York, 1978).

[18] B.Z. Kopeliovich, J. Nemchick, N.N. Nikolaev and B.G. Zakharov, Phys. Lett. **B324** 1994.

[19] V. Franco and R.J. Glauber, Phys. Rev. **142** (1966) 1195.

[20] L. Bertocchi and A. Capella, Il Nuovo Cimento **A51** (1967) 369.

[21] M. Arneodo et al., Nucl. Phys. **B429** (1994) 503; M. Derrick et al., Phys. Lett. **B356** (1995) 601; S. Aid et al., Nucl. Phys. **B468** (1996) 3.

[22] L.L. Frankfurt, W.R. Greenberg, G.A. Miller, M. Sargsian and M.I. Strikman, Phys. Lett. **B369** (1996) 201.

[23] B.L. Ioffe, Phys. Lett. **30** (1968) 123.

[24] M. Arneodo, Phys. Rep. **240** (1994) 301.

[25] G.E. Brown and A.D. Jackson, *The Nucleon-Nucleon Interaction* (North-Holland, Amsterdam, 1976).

[26] E.V. Shuryak, Rev. Mod. Phys. **65** (1993) 1.

[27] L.L. Frankfurt and M.I. Strikman, Nucl. Phys. **B250** (1985) 143.

[28] S. Godfrey and N. Isgur, Phys. Rev. **D32** (1985) 189.

Figure Captions:

Figure 1:
The cross section ratio R_δ from Eq.(16) for photoproduction (a) for various values of ν. R_δ for leptoproduction (b) for various values of Q^2.

Figure 2:
The differential cross section $d\sigma^{\parallel}_{\gamma N}/dt$ for the photoproduction of ρ mesons off deuterons polarized parallel to the photon momentum. The solid curves show results from vector meson dominance using proper longitudinal interaction lengths (14,15). The dashed lines correspond to a longitudinal interaction length $\delta_1 \sim |1/l_z|$ instead of $\delta_1 \sim |1/l_-|$. In both cases the cross sections decrease for increasing photon energies.

Figure 3:
The Q^2-dependence of the cross section ratio R_{ct} from Eq.(18) for various values of t. The full line corresponds to vector meson dominance. The dashed curve results from the application of color diffusion to longitudinally and transversely polarized photons. For the dot-dashed lines color diffusion has been applied to longitudinal photons only. In this case the photon polarization parameter has been fixed at $\varepsilon = 0.5$.

Figure 4:
The Q^2-dependence of the cross section ratio for coherent ρ production from unpolarized deuterons taken at $t = -0.8$ and $-0.4\,GeV^2$. The solid line represents the complete vector meson dominance calculation. The dashed curve accounts for the Born contribution only. The shaded area exhibits results from quantum diffusion (12). The characteristic expansion time $\tau_f = 2\nu/\delta m_\rho^2$ has been varied via $\delta m_\rho^2 = (0.7 - 1.1)\,GeV^2$.

Figure 5:
The cross section $d\sigma^{\perp}_{\gamma^* N}/dt$ normalized to its value at $t = t_{min}$ for various values of Q^2 and fixed $x = 0.1$. The solid lines present the complete vector meson dominance calculation. Results from quantum diffusion are shown by the dashed curves. At $t \simeq -0.4\,GeV^2$ both cross sections decrease with rising values of Q^2. The arrow indicates the position of the node in the Born contribution.

Figure 6:
The tensor polarization asymmetry A_d from (20) for various values of Q^2 and fixed $x = 0.1$. The spin quantization axis has been chosen either perpendicular to the vector meson production plane (a), or parallel to the photon momentum (b). The solid lines show the complete vector meson dominance calculation. The dotted curve represent the Born

contributions. Results from quantum diffusion are shown by the dashed curves. At $-t > 0.4\,GeV^2$ the curves to the right correspond to increasing values of Q^2.

Figure 7:
The t-dependence (a) of the ϕ photoproduction cross section $d\sigma^{\perp}_{\gamma N}/dt$ normalized to its value at $t = t_{min}$ for different values of the ϕ-nucleon cross section $\sigma_{\phi N} = 15$ (full) and $10\,mb$ (dashed). The photon energy is fixed at $\nu = 6\,GeV$. In (b) the ratio of both cross sections is shown.

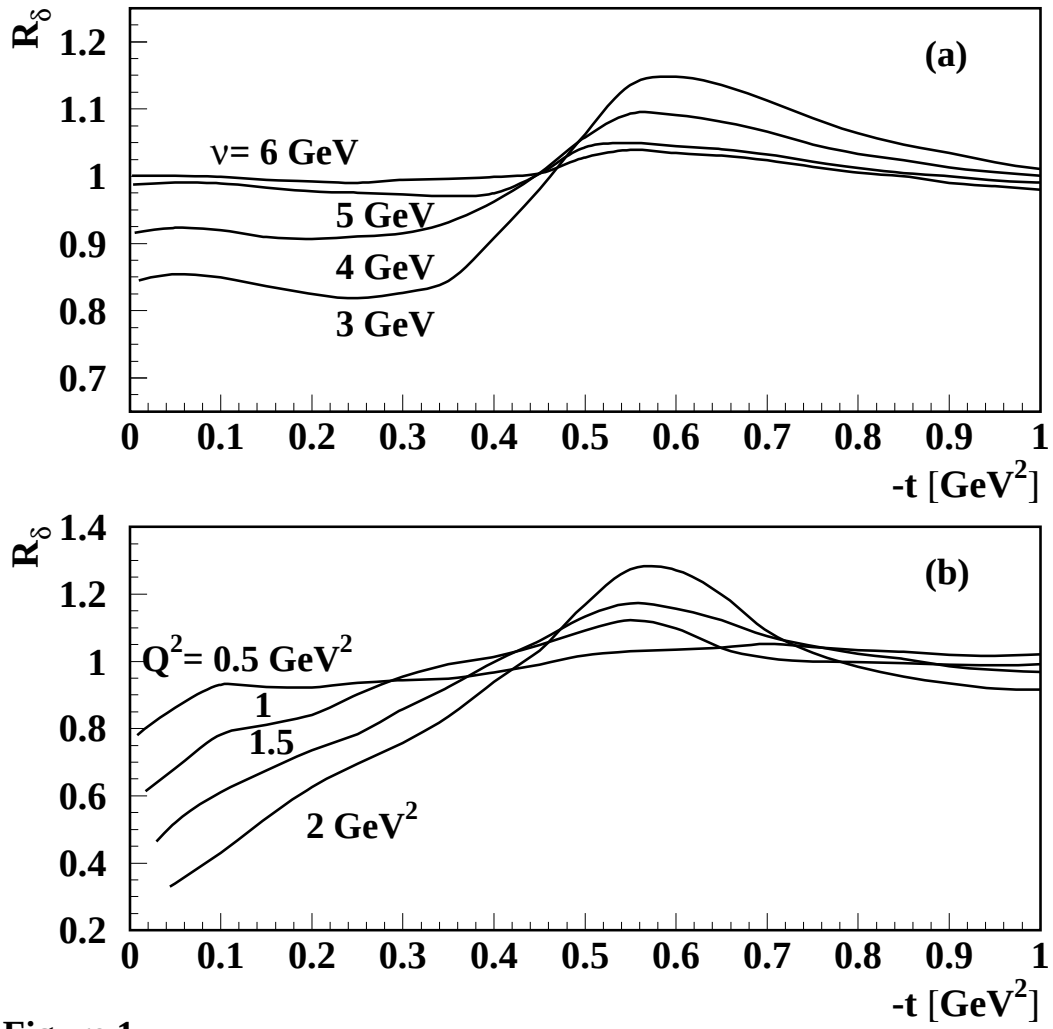

Figure 1

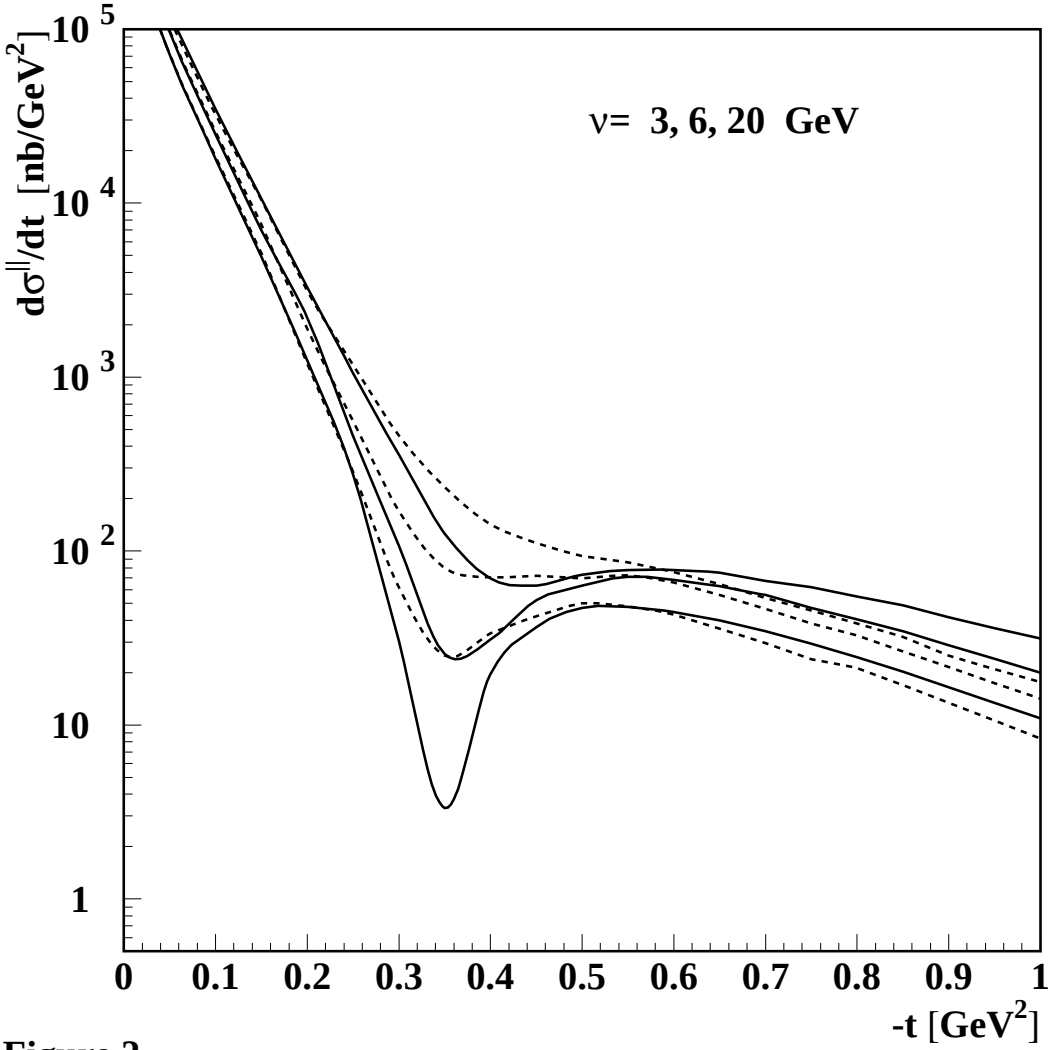
ν= 3, 6, 20 GeV
dσ||/dt [nb/GeV2]
10 5
10 4
10 3
10 2
10
1
0
0.1
0.2
0.3
0.4
0.5
0.6
0.7
0.8
0.9
1
-t [GeV2]

Figure 2

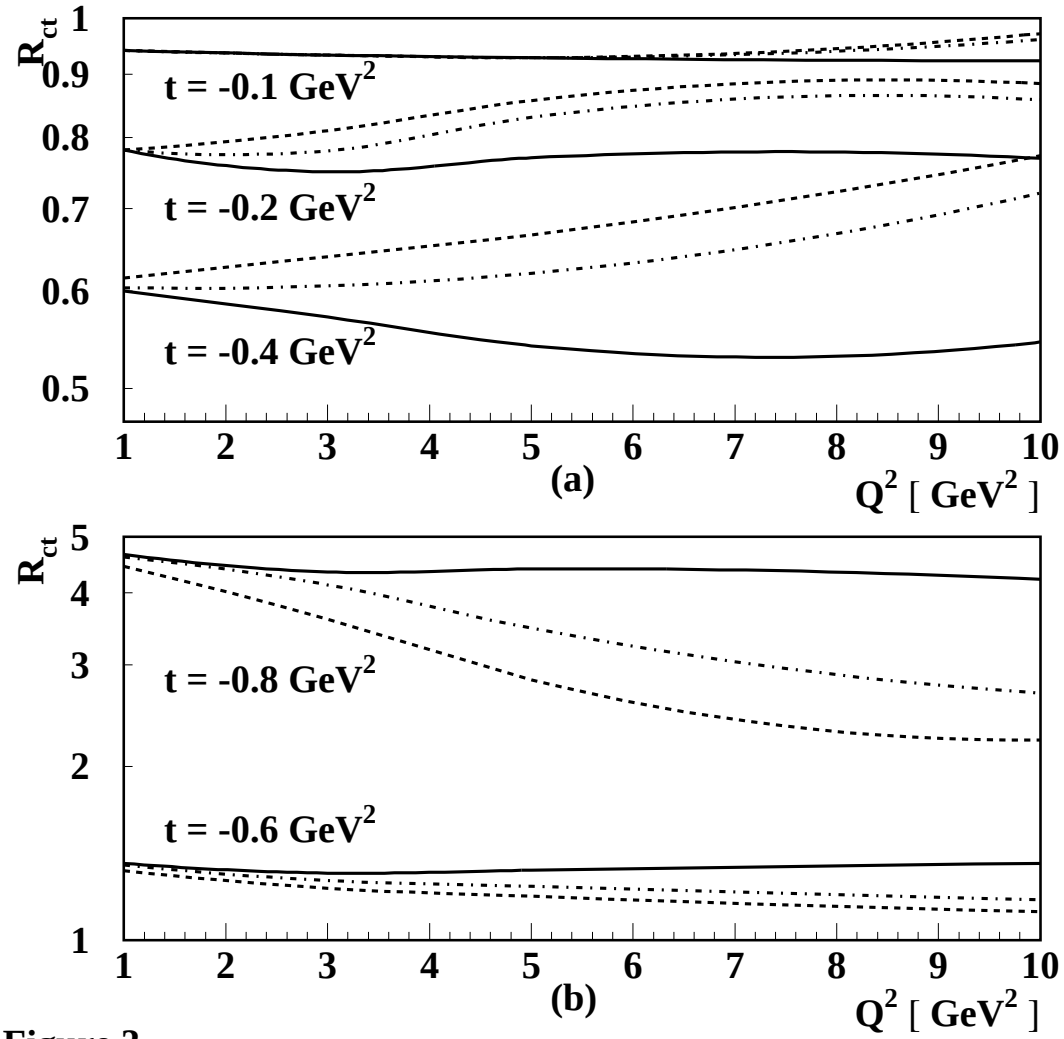
R_ct
1
0.9
0.8
0.7
0.6
0.5
t = -0.1 GeV^2
t = -0.2 GeV^2
t = -0.4 GeV^2
1 2 3 4 5 6 7 8 9 10
(a)
Q^2 [GeV^2]
R_ct
5
4
3
2
1
t = -0.8 GeV^2
t = -0.6 GeV^2
1 2 3 4 5 6 7 8 9 10
(b)
Q^2 [GeV^2]

Figure 3

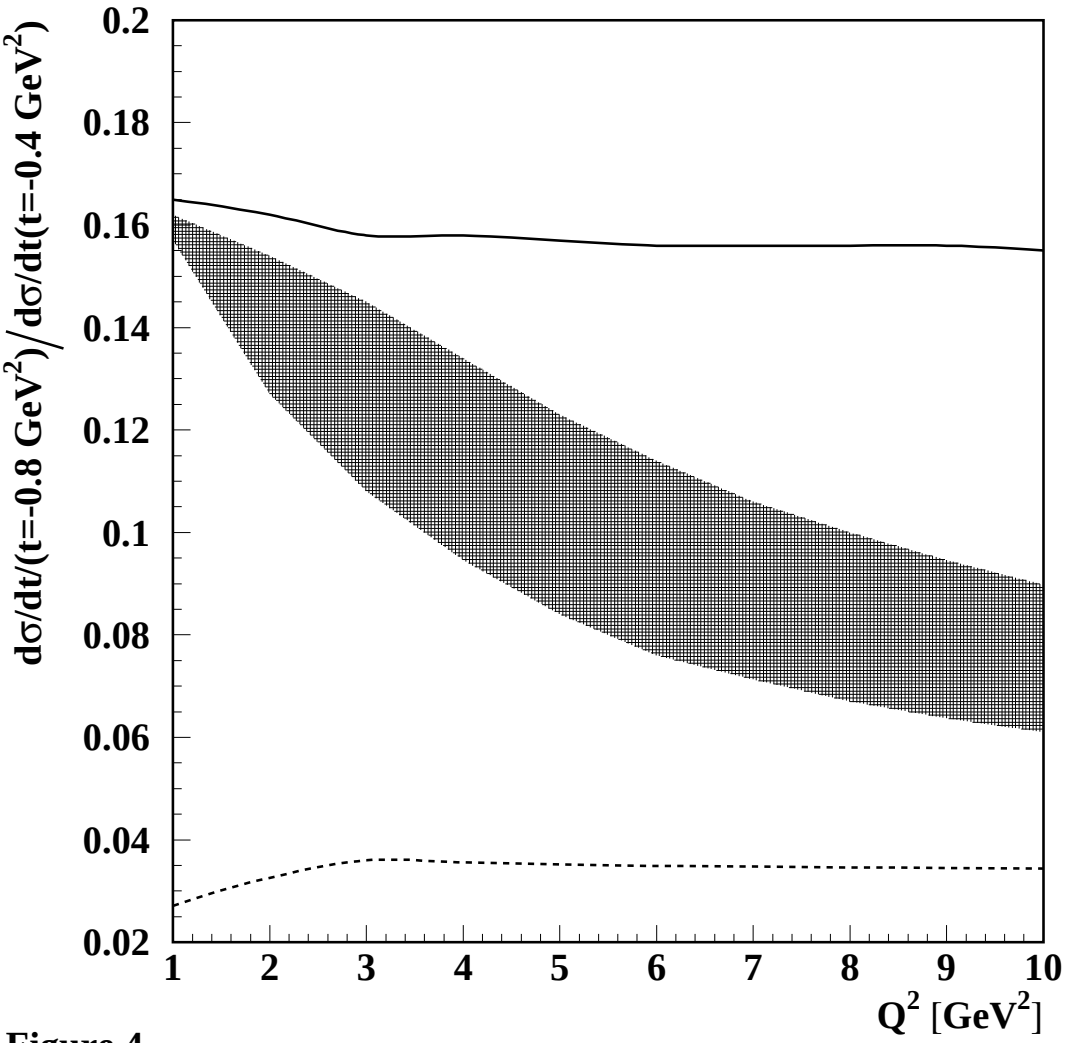
0.2
0.18
0.16
0.14
0.12
0.1
0.08
0.06
0.04
0.02
1
2
3
4
5
6
7
8
9
10
Q^2 [GeV^2]
$d\sigma/dt/(t=-0.8\ GeV^2)\big/d\sigma/dt(t=-0.4\ GeV^2)$

Figure 4

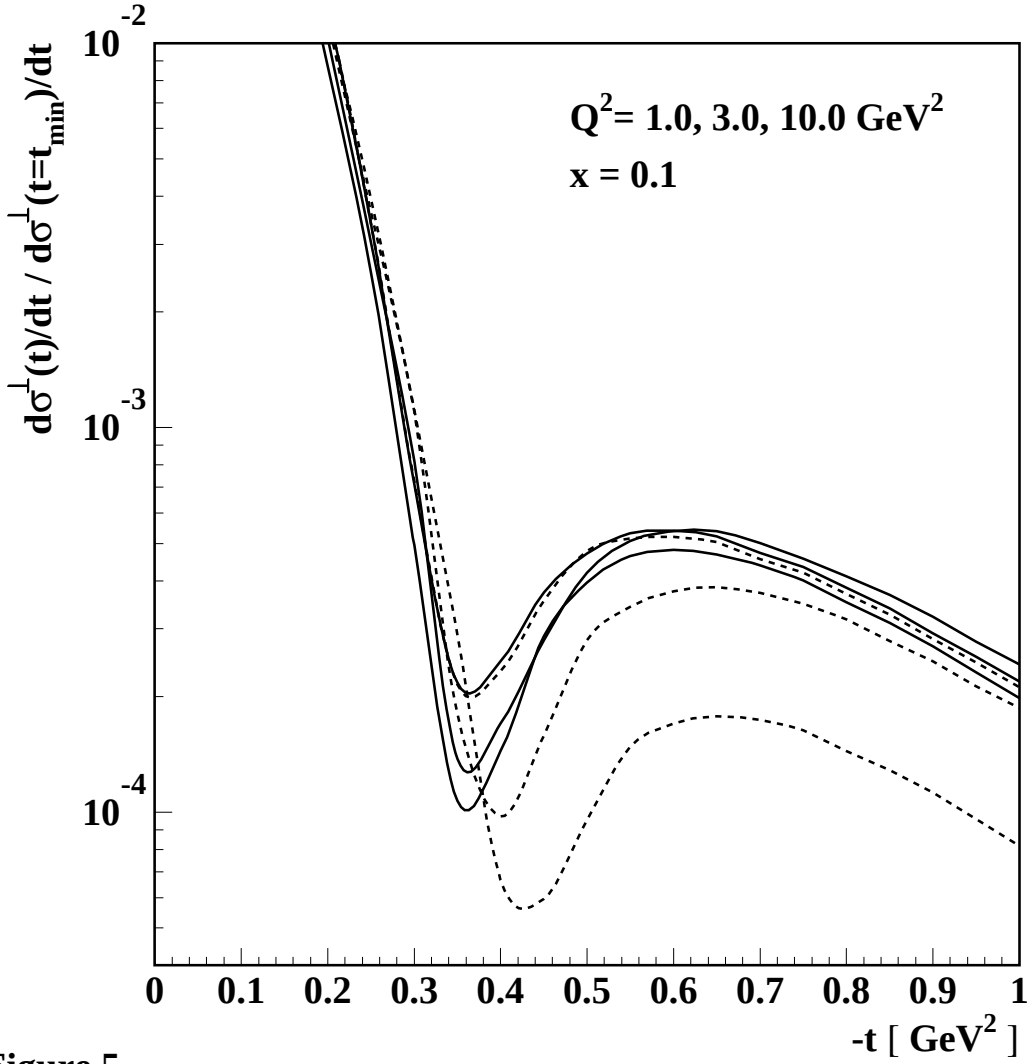
10^{-2}
10^{-3}
10^{-4}
$d\sigma^{\perp}(t)/dt\ /\ d\sigma^{\perp}(t=t_{min})/dt$
Q^2= 1.0, 3.0, 10.0 GeV^2
x = 0.1
0
0.1
0.2
0.3
0.4
0.5
0.6
0.7
0.8
0.9
1
-t [GeV^2]

Figure 5

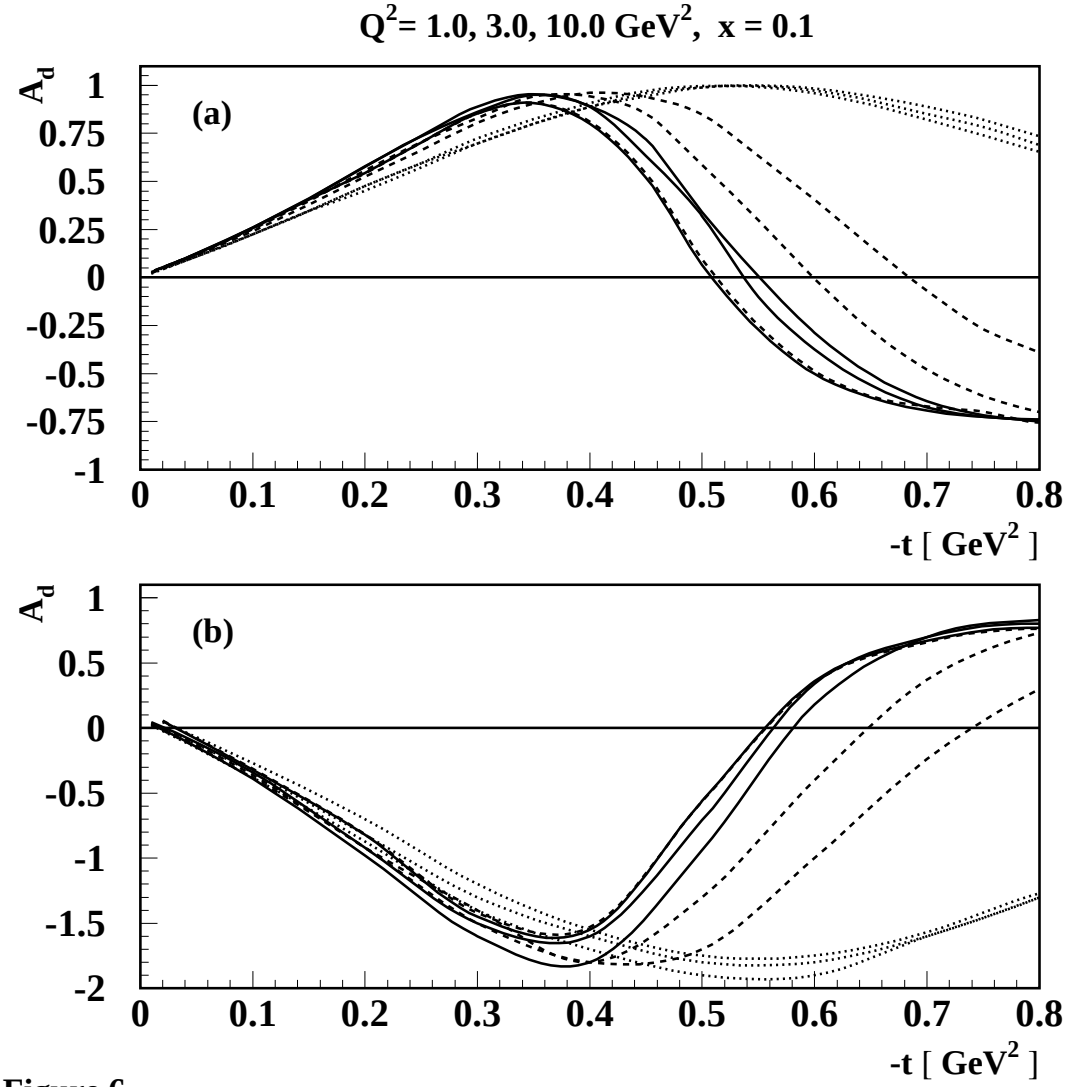
Q^2= 1.0, 3.0, 10.0 GeV^2, x = 0.1
A_d
(a)
1
0.75
0.5
0.25
0
-0.25
-0.5
-0.75
-1
0
0.1
0.2
0.3
0.4
0.5
0.6
0.7
0.8
-t [GeV^2]
A_d
(b)
1
0.5
0
-0.5
-1
-1.5
-2
0
0.1
0.2
0.3
0.4
0.5
0.6
0.7
0.8
-t [GeV^2]

Figure 6

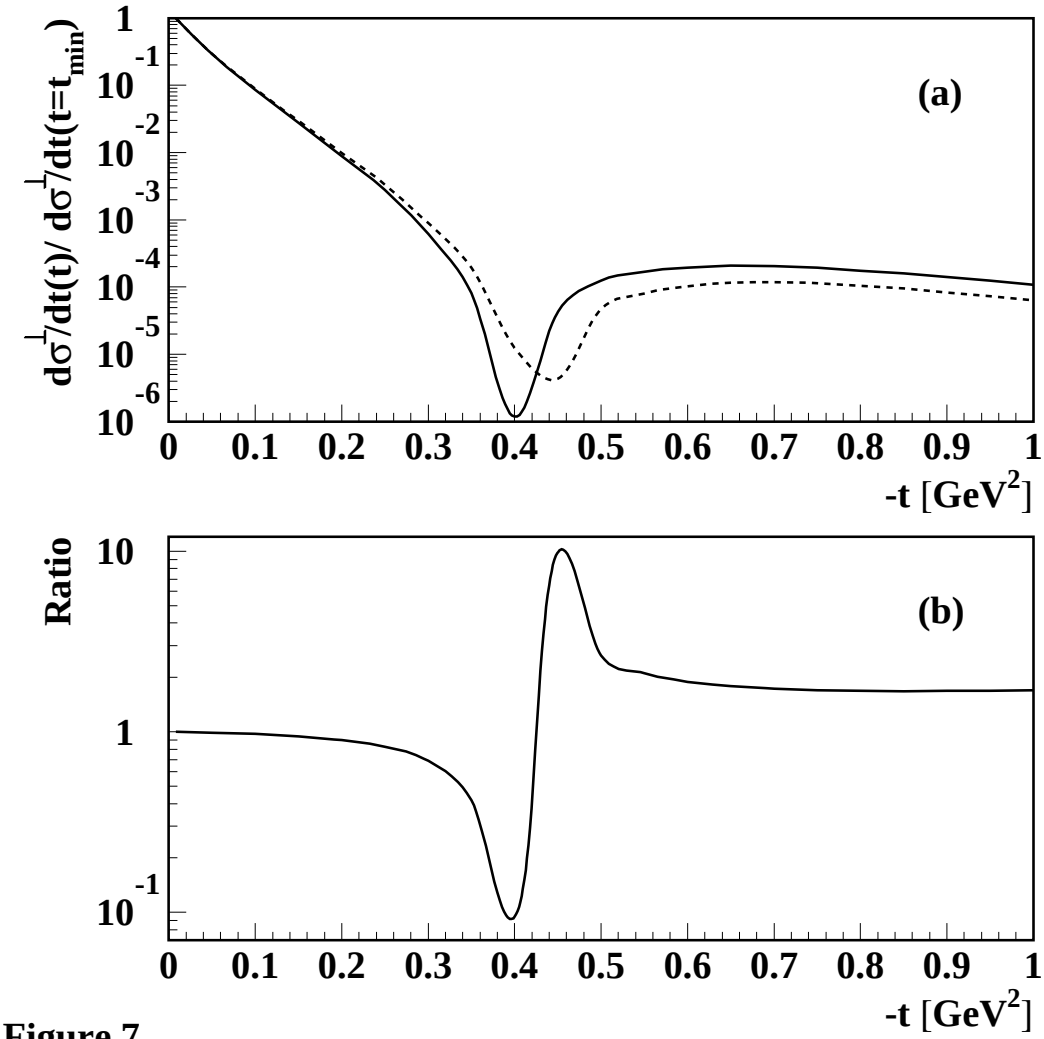

Figure 7